

field boundary condition corresponds for proper drag predictions. Rudy and Strikwerda (1980) in solving the Navier-Stokes equations at subsonic flow introduced a pressure based boundary condition. Since the information is propagated along the characteristic paths, Zamzamian and Razavi (2008) declared that the multi-dimensional characteristic based (MCB) scheme takes into account the real two-dimensional nature of flow, and ensure accuracy and convergence of the simulations. Hashemi and Zamzamian (2014) investigated far field boundary condition implementation in the incompressible flow. They presented (MCB) for artificial compressibility (AC) equations, to evaluate the flow variables at the far field boundary. They found that the conventional far field boundary estimation for incompressible flows will cause reflected waves to be returned back to the computational domain and delay the solution to steady state. Razavi *et al.* (2008) have proposed a genuine multidimensional upwind scheme for solving the incompressible flows. This idea also will be employed in boundary modeling. Bayliss and Turkel (1982) used the outgoing waves in two and three dimensional spaces and proposed a pressure based formulation. Their boundary condition is applicable for Euler and Navier Stokes equations. Giles (1990) presented linearized boundary conditions based on the characteristics of two dimensional Euler equations by Fourier analysis. Verhoff (1988) used two dimensional Euler equations in streamlined coordinates in terms of linearized Riemann variables. Then, he applied Fourier analysis for boundary condition treatment. Roe (1989) proved that some convenient boundary conditions are incorrect and then for the Euler equations by using bicharacteristic analysis on acoustic waves introduced boundary conditions based on wave angle. Razavi (1997) formulated the Euler equations in terms of the Riemann variables along with asymptotic expansions of Riemann variables based on wave propagation theory. The major interest of all researches has been the modification of convergence rate, or reducing the computational domain. Based on the characteristic theorem, there is no problem in imposing boundary conditions for supersonic flows (Razavi (1997)). However, in subsonic and transonic flows, imposing the boundary conditions should be done by a characteristic manner, because in the computational domain, propagation of information takes place along specific paths. Inflow and outflow boundary conditions that are a kind of far field boundaries, from one side are influenced by computational domain and from another side with the outer zone which usually assumes free stream conditions. Thus, an inflow or outflow boundary is subject to two types of numerical information that hit the boundary. It has been shown by Karni (1991) that if this incidence does not happen along the characteristic paths, the information received by the boundary, reflects back into the computational domain and yields in the numerical instability. Some of past boundary models have major problems. In two dimensional flows the one dimensional characteristics have been used which requires to locate the boundaries very far from the

nonlinear zone or in other cases complicated relations have been used.

Here, a genuine multidimensional approach for boundary treatment is offered which is mainly based on the formulation derived by Razavi (1995). This treatment takes into account the multidirectional wave propagation at the inflow and outflow boundaries.

2. WAVE PROPAGATION MODEL

The two dimensional Euler equations in quasi linear form are expressed as

$$\frac{\partial U}{\partial t} + A \frac{\partial U}{\partial x} + B \frac{\partial U}{\partial y} = 0, \quad (1)$$

Where

$$U = \begin{bmatrix} \rho \\ u \\ v \\ p \end{bmatrix}, \quad A = \begin{bmatrix} u & \rho & 0 & 0 \\ 0 & u & 0 & \frac{1}{\rho} \\ 0 & 0 & u & 0 \\ 0 & \gamma p & 0 & u \end{bmatrix}, \quad B = \begin{bmatrix} v & 0 & \rho & 0 \\ 0 & v & 0 & 0 \\ 0 & 0 & v & \frac{1}{\rho} \\ 0 & 0 & \gamma p & v \end{bmatrix}.$$

In partial differential equations, the fronts of propagating waves can be represented by characteristic surfaces (Razavi (1995)), and compatibility relations for equation (1) after some algebraic manipulations become:

$$\begin{aligned} \left[\pm a \sqrt{\left(\frac{\partial f}{\partial x}\right)^2 + \left(\frac{\partial f}{\partial y}\right)^2} \right] du + \frac{dp}{\rho} + \frac{\partial f}{\partial x} &= 0, \\ \left[\pm a \sqrt{\left(\frac{\partial f}{\partial x}\right)^2 + \left(\frac{\partial f}{\partial y}\right)^2} \right] dv + \frac{dp}{\rho} + \frac{\partial f}{\partial y} &= 0. \end{aligned} \quad (2)$$

By assuming the following relations for the wave directions:

$$\cos \phi = \frac{\frac{\partial f}{\partial x}}{\sqrt{\left(\frac{\partial f}{\partial x}\right)^2 + \left(\frac{\partial f}{\partial y}\right)^2}}, \quad \sin \phi = \frac{\frac{\partial f}{\partial y}}{\sqrt{\left(\frac{\partial f}{\partial x}\right)^2 + \left(\frac{\partial f}{\partial y}\right)^2}} \quad (3)$$

One gets:

$$\begin{aligned} \pm du + \cos \phi \frac{dp}{\rho a} &= 0, \\ \pm dv + \sin \phi \frac{dp}{\rho a} &= 0. \end{aligned} \quad (4)$$

Hence, Eq. (2) can be recast as the following multi-dimensional characteristic relations. Integrating the Eq. (4) results in the Riemann variables in a special form:

$$\begin{aligned} R_u &= u + \cos \phi \frac{2}{\gamma - 1} a, & Q_u &= u - \cos \phi \frac{2}{\gamma - 1} a, \\ R_v &= v + \sin \phi \frac{2}{\gamma - 1} a, & Q_v &= v - \sin \phi \frac{2}{\gamma - 1} a. \end{aligned} \quad (5)$$

We call these quantities the projected Riemann variables, which will be used in boundary condition formulation. They are shown in Figure 1. In cartesian coordinates R_u and Q_u are parallel to x-axis while R_v and Q_v parallel to y-axis. For inclined boundaries ($\theta \neq \pi/2$), the normal and

tangential Riemann variables are used as shown in Figure 2. In this figure for inflow boundary, R_u and Q_v quantities are computed from out of the computational domain and R_v and Q_u from inside the domain. In other words R_u and Q_v are carrying information from free stream and R_v and Q_u are carrying information from the computational cells

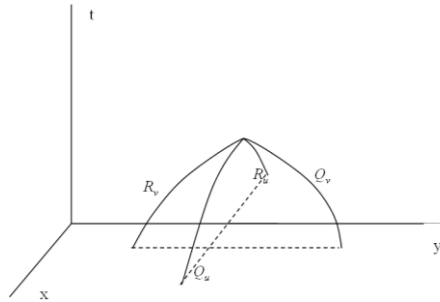


Fig. 1. Projected Riemann variables in time-like (x,y,t) coordinates.

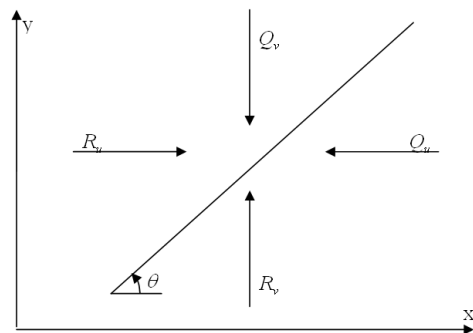


Fig. 2. Location of projected Riemann variables in two-dimensional space.

3. BOUNDARY CONDITIONS MODELING

In general the inflow and outflow boundaries are subject to two kinds of information: (a) information propagating from outside of boundary towards the boundary; (b) information propagating from computational domain to the boundary. Overly, it is believed that any kind of information is brought to the boundary along the characteristic paths. The information can be classified into two types, namely physical and numerical. The physical information arises from the nature of equations. Here, in our case, the Euler equations under conditions can be recast into wave equations. The numerical information or error waves are motivated due to discretization process. In finite volume method, each cell side was hit by several waves. Boundaries from one side are exposed to outside information and from other side receive information from the inner cells. For inflow and outflow boundary modeling the projected Riemann variables (5) are used. The wave directions that reach to the boundary are responsible for information exchange between the domain and outside world. The wave

direction ϕ , can be determined from Eq. (4) as following:

$$\tan \phi = \frac{dv}{du} = \frac{dv/dt}{du/dt}. \quad (6)$$

We attempt to find a physically-based way for approximating the ϕ directions. In semi-discretized form, the relation (6) can take the following form:

$$\phi = \arctan \frac{\Delta v / \Delta t}{\Delta u / \Delta t}. \quad (7)$$

When the inflow and outflow boundaries are almost perpendicular to the free stream direction, the Riemann variables take the following form:

$$R_u = u + \cos \phi \frac{2}{\gamma - 1} a, \quad Q_u = u - \cos \phi \frac{2}{\gamma - 1} a \quad (8)$$

In relation (8), the ϕ can take any value between zero and π . For inflow boundary R_u is computed from outside and Q_u from inside the domain. The angle ϕ is obtained using Eq. (7). Then u and a can be computed considering the following relations.

$$u^{n+1} = \frac{1}{2} (R_u^{n+1} + Q_u^{n+1}), \quad (9)$$

$$a^{n+1} = \frac{\gamma - 1}{4 \cos \phi} (R_u^{n+1} - Q_u^{n+1}).$$

To calculate v , the R_v and Q_v are used in a similar fashion. Now, having these three parameters known, the other flow parameters at inflow boundary are calculated by the following manner:

$$\rho_{in} = \left[\left(\rho_{\infty}^{\gamma} a_{in}^2 \right) / \left(\gamma p_{\infty} \right) \right]^{\frac{1}{\gamma - 1}}, \quad p_{in} = \frac{\rho_{in} a_{in}^2}{\gamma}, \quad (10)$$

$$e_{tin} = p_{in} / \left[\rho_{in} (\gamma - 1) \right] + \frac{1}{2} \left(u_{in}^2 + v_{in}^2 \right).$$

After completing these calculations, the flow parameters at inflow boundary can be obtained and joined to the flow solver. The outflow boundary modeling is performed in a similar manner. However, in this case, R_u from inside and Q_u from outside of the domain can be obtained.

4. EVALUATION OF THE PROPOSED BOUNDARY MODEL

For evaluating this model in isentropic compressible internal flow an inhouse FORTRAN90 code has been written. Flow regime includes the subsonic and transonic regimes. A circular arc bump channel with an arc having ten percent of its chord, and length of three chords is used. The generated grid is structured and elliptic. At first the channel with dimensions mentioned above and a channel with reduced length was analyzed. In these cases the conventional boundary conditions have been used. The length of reduced channel is 1.2 of the chord. To validate the results, the Mach number and pressure coefficient at cells near the down wall in extended channel is compared with the results of other investigators. Mach number and pressure coefficient variations in subsonic flow with conventional boundary

conditions in extended and reduced channels are shown in Figure 3 and Figure 4.

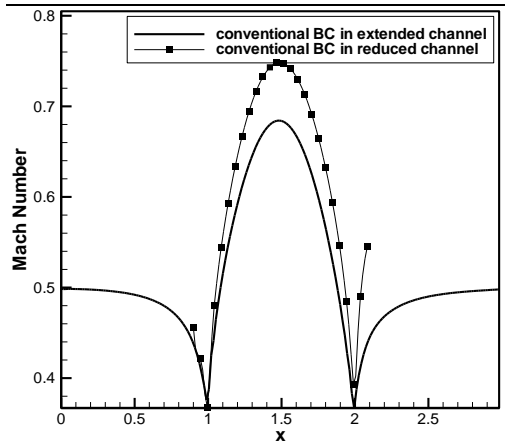


Fig. 3. Mach number in extended and reduced channels with conventional BC, $M_{in}=0.5$, $CFL=3$.

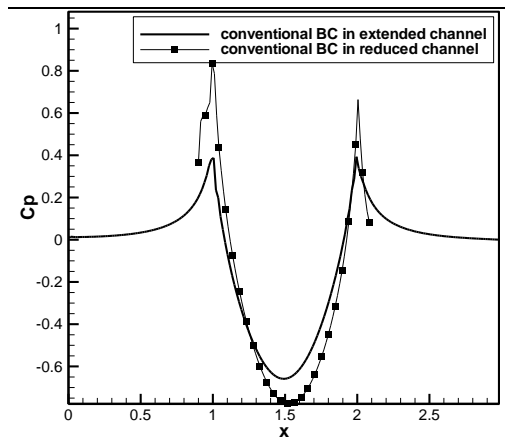


Fig. 4. Pressure coefficient in extended and reduced channels with conventional BC, $M_{in}=0.5$, $CFL=3$.

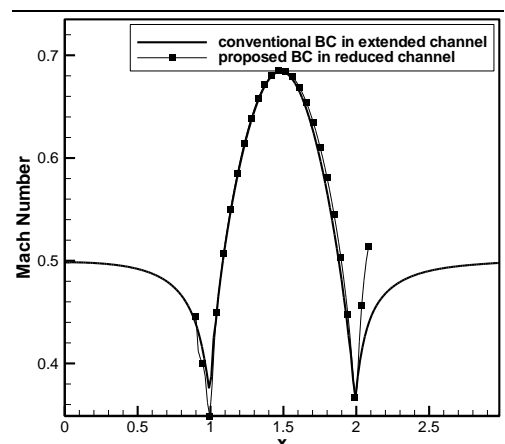


Fig. 5. Mach number in extended channel with conventional BC and in reduced channel with proposed BC, $M_{in}=0.5$, $CFL=3.5$.

Then in reduced channel the proposed model is applied. Plots for this case with results of extended channel for comparison are shown in Figure 5 and

Figure 6.

For transonic flow also these results have been obtained and displayed in Figures 7-10

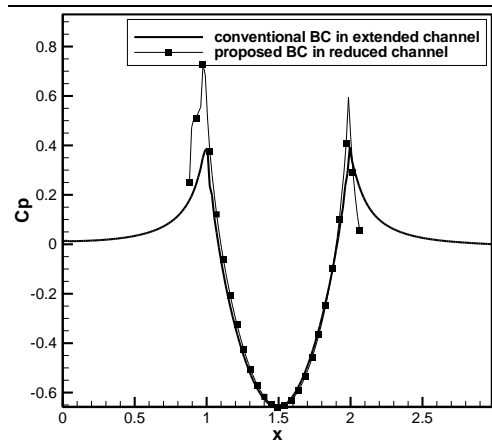


Fig. 6. Pressure coefficient in extended channel with conventional BC and in reduced channel with proposed BC, $M_{in}=0.5$, $CFL=3.5$.

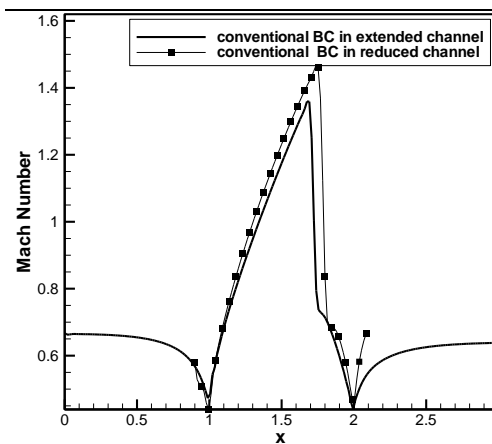


Fig. 7. Mach number in extended and reduced channels with conventional BC, $M_{in}=0.675$, $CFL=4$.

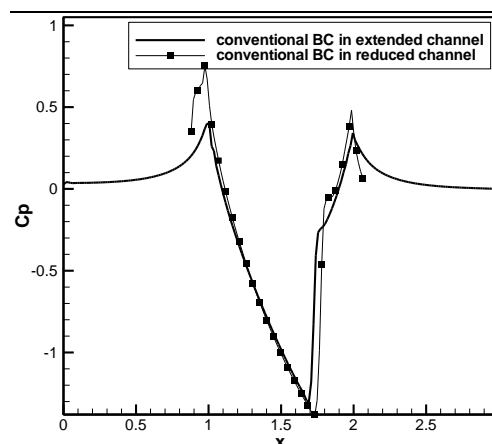


Fig. 8. Pressure coefficient in extended and reduced channels with conventional BC, $M_{in}=0.675$, $CFL=4$.

The convergence histories are shown in Fig. 11-14. The extended channel has 190×20 cells and the reduced channel consist of 76 cells along the length. From Figs. 3, 4, 7 and 8 it is seen that by putting the boundaries close to the nonlinear zone, here the arc bump, with conventional boundary conditions, there is a considerable difference between extended and reduced channel results. This is due to the inefficiency of conventional boundary conditions when the boundaries are close to the nonlinear regions. But in Figures 5, 6, 9, and 10 it can be obtained that there is a good agreement between the extended channel with conventional model and reduced channel with the proposed model results. In Figures 11 and 12 one can see that with the proposed model the convergence process is accelerated. By the aid of the proposed model for inflow and outflow boundaries we have been able to locate the boundaries very close to the nonlinear zone while keeping the accuracy. By this model the number of numerical cells was reduced to 1/3 that has a substantial effect on the number of calculations and convergence time.

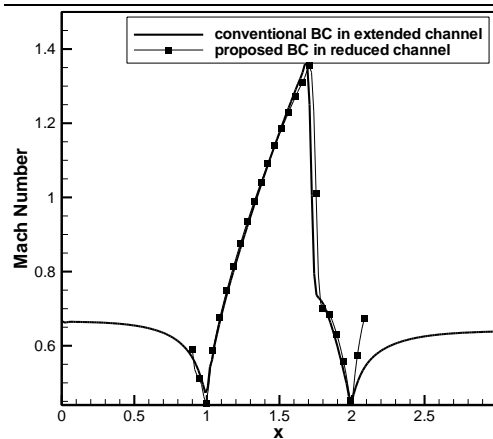


Fig. 9. Mach number in extended channel with conventional BC and in reduced channel with proposed BC, $M_{in}=0.675$, $CFL=4.5$.

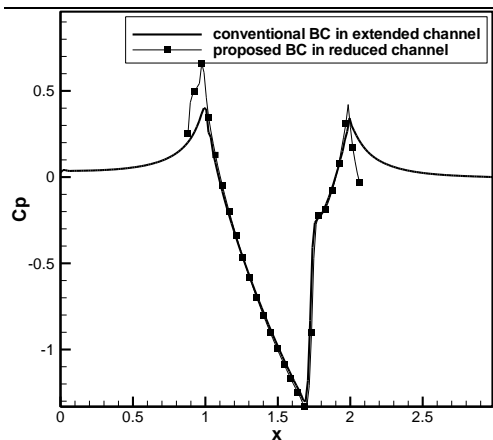


Fig. 10. Pressure coefficient in extended channel with conventional BC and in reduced channel with proposed BC, $M_{in}=0.675$, $CFL=4.5$.

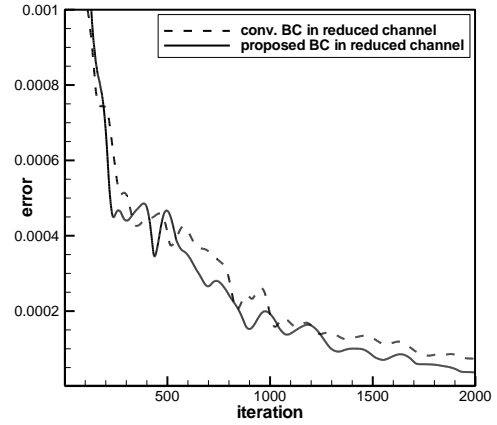


Fig. 11. Comparison of convergence histories in reduced channel with conventional and proposed BCs, $M_{in}=0.5$, $CFL=3$.

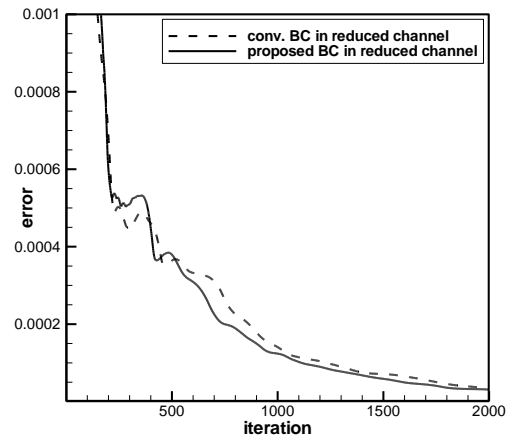


Fig. 12. Comparison of convergence histories in reduced channel with conventional and proposed BCs, $M_{in}=0.675$, $CFL=4$.

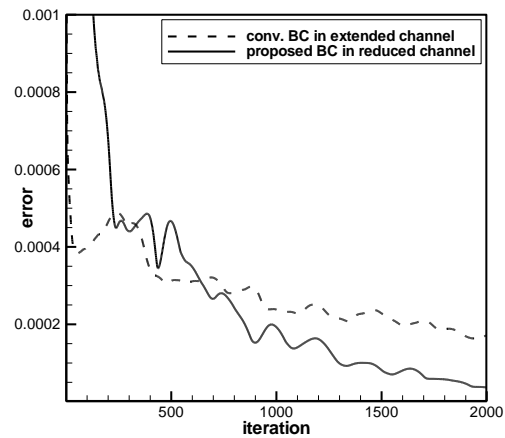


Fig. 13. Comparison of convergence histories in reduced channel with conventional and in extended channel with proposed BCs, $M_{in}=0.5$, $CFL=3$.

As it is observed from Figures 15 and 16 a periodic pattern for propagation angle φ would exist. This behavior is of interest and can be considered in boundary condition modeling.

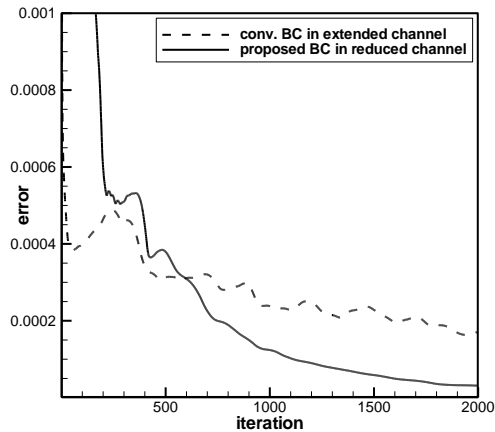


Fig. 14. Comparison of convergence histories in reduced channel with conventional and in extended channel with proposed BCs, $M_{in}=0.675$, $CFL=4$.

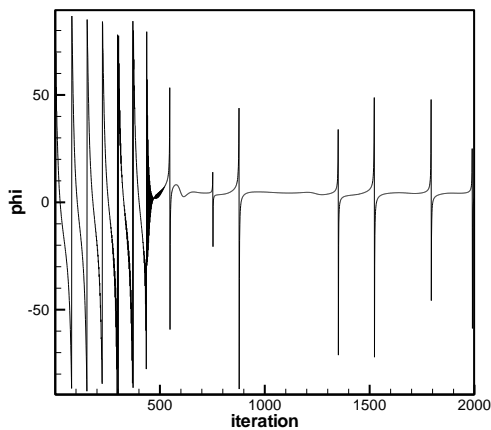


Fig. 15. Diagram of φ angle in a cell of inflow boundary

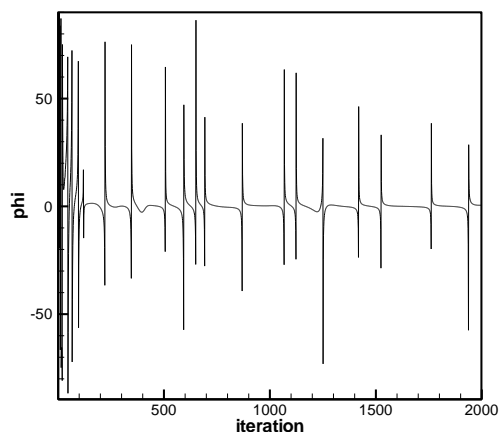


Fig. 16. Diagram of φ angle in a cell of outflow boundary.

5. CONCLUSION

A novel characteristic formulation of the Euler equations has been shown in this paper. The projected Riemann variables are derived based on

the wave propagation direction, φ . Numerical experiments with wave angle φ confirmed that this angle exhibits a periodic behavior near the inflow and outflow boundaries. The projected Riemann variables were consistently adopted and used in the boundary condition formulations. This new multi-dimensional characteristic-based model resulted in reducing the convergence steps to steady state and saving the memory requirements. It can conveniently be extended to three-dimensional flows.

REFERENCES

- Bayliss, A., and E. Turkel. (1982). Outflow Boundary Condition for Fluid Dynamics. *SIAM Journal on Scientific Computing* 3(2).
- Giles, M. B. (1990). Nonreflecting Boundary Conditions for Euler Equation Calculations. *AIAA J* 28(12).
- Hashemi, M. Y., K. Zamzamian (2014). Efficient and non-reflecting far-field boundary conditions for incompressible flow calculations. *Applied Mathematics and Computation* 230, 248–258.
- Holst, T. L., J. Flonas, U. Kaynak and N. M. Chaderjian (1990). Navier–Stokes computations about complex configurations including a complete F-6 aircraft. *Applied Computational Aerodynamics* 125.
- Jameson, A., W. Schmidt and E. Turkel (1981). Numerical solution of the Euler equations by finite volume methods using Runge-Kutta time stepping schemes. *AIAA 14th Fluid and Plasma Dynamics Conference AIAA* 15p.
- Karni, S. (1991). To the Boundary and Back-a Numerical Study. *International Journal for Numerical Methods in Fluids* 13, 201-216.
- Parameswaran, S., R. Andra, R. Sun and M. Gleason (1997). Critical study on the influence of far field boundary conditions on the pressure distribution around a bluff body. *Journal of Wind Engineering and Industrial Aerodynamics* 67& 68, 117-127.
- Razavi, S. E. (1997). *Far-Field Boundary Conditions for Computation of Internal Compressible Flows*. *Journal of Faculty of Engineering* 15, In Persian.
- Razavi, S. E. (1995). *Far Field Boundary Conditions for Computation of Compressible Aerodynamic Flows*. Ph. D. thesis, Department of Mechanical Engineering, McGill University Montreal Canada.
- Razavi, S. E., K. Zamzamian and A. Farzadi (2008). *Genuinely Multidimensional Characteristic-Based Scheme for Incompressible Flows*. *International Journal for Numerical Methods*

- in Fluids* 57, 929-949.
- Roe, P. L. (1989). Remote Boundary Conditions for Unsteady Multidimensional Aerodynamic Computations. *Computers & Fluids* 17(1), 221–231.
- Rudy, D. H. and J. C. Strikwerda (1980). A Nonreflecting Outflow Boundary Condition for Subsonic Navier–stokes Calculations. *Journal of Computational Physics* 36, 55-70.
- Verhoff, A. (1988). *Far Field Computational Boundary Conditions for Internal Flow Problems*. Naval Postgraduate School, Monterey, California.
- Zamzamian, K., S. E. Razavi (2008). Multidimensional upwinding for incompressible flows based on characteristics, *Journal of Computational Physics* 227, 8699–8713.